Ultrafast X-ray scattering from a laser-driven MgO crystal.

V. Guskov[1,2]

supervised by D. Gorelova[2]

[1] *Moscow Institute of Physics and Technology, Institutskiy per. 9, Dolgoprudny, 141701, Russian Federation*
[2] *Center for Free-Electron Laser Science, DESY, Notkestrasse 85, D-22607 Hamburg, Germany*

Abstract

We study ultrafast x-ray scattering from a laser-driven MgO crystal that provides us an information about electronic structure of the laser-driven crystal. Relying on a derived theoretical description of the light-matter interaction and calculating scattering spectra, we analyze how the results depend on essential parameters of the driving laser pulse and the probe x-ray pulse.

September 6, 2018

Contents

1 Introduction

In order to understand different processes in atoms, molecules and materials, different techniques are used including light scattering. There is a growing interest in probing microscopic details of light-matter interaction. For this reason, we consider x-ray scattering from the cubic wide-bandgap MgO crystal affected by an optical electromagnetic field. We study a process, in which the electronic system of the crystal under the influence of an optical pump pulse, is probed by means of x-ray scattering. This provides us information about the excited electronic structure of the solid.

In the present work, we study how a scattering signal depends on properties of the x-ray and the optical pulses. First, the dependence of the signal on pump pulse polarization, intensity and frequency are demonstrated. Second, we show how the probe pulse duration affects the scattering signal.

The pump pulse is an intensive electromagnetic field with the photon energy of 1.55 eV that excites the electronic system. The interaction between the pump pulse and the electronic system is described within the Floquet-Bloch theory. The probe pulse with the photon energy of several keV has a Gaussian shape. The interaction between the probe pulse and the electronic system is described within the first-order perturbation theory.

2 Theory of X-ray scattering from laser-driven system

The interaction between the electronic system of the MgO crystal and the optical single-mode electromagnetic filed is described in a nonperturbative way using the Floquet-Bloch approach [1],[2]. We refer to a laser-driven system as an electronic system entangled to the optical laser field. We treat the x-ray pulse within the first-order perturbation theory. Within the perturbation theory we obtain the probabilities to scatter a photon with an initial wave-vector $\mathbf{k}_{\text{in}}$ to the state with a final wave-vector $\mathbf{k}_{\text{st}}$.

2.1 Pump pulse

The Hamiltonian of a laser-driven (LD) system describing the interaction between the electronic system and a single-mode electromagnetic field is

$$\hat{H}_{LD} = \hat{H}_{el} + \hat{H}_{em} + \hat{H}_{int}, \tag{1}$$

$$\hat{H}_{em} = \omega \hat{a}^{\dagger}_{\boldsymbol{\kappa}_0,s_0} \hat{a}_{\boldsymbol{\kappa}_0,s_0}, \tag{2}$$

$$\hat{H}_{int} = \frac{1}{c} \int d^3\mathbf{r} \hat{\psi}^{\dagger}(\mathbf{r})(\hat{\mathbf{A}}(\mathbf{r})\hat{\mathbf{p}})\hat{\psi}(\mathbf{r}). \tag{3}$$

Here, $\hat{H}_{el}$ is the Hamiltonian of the electronic system, $\hat{H}_{em}$ is the Hamiltonian of the electromagnetic field, and $\hat{H}_{int}$ describes the interaction between the electromagnetic field and the electronic system. $\hat{a}^{\dagger}_{\boldsymbol{\kappa},s}$ ($\hat{a}_{\boldsymbol{\kappa},s}$) creates (annihilates) a photon with wave vector $\boldsymbol{\kappa}$ and polarization s. We assume that only $\boldsymbol{\kappa}_0, s_0$ mode with corresponding polarization vector ϵ_0 and the energy $\omega = |\boldsymbol{\kappa}_0|c$, where c is the speed of light, is occupied. $\hat{\mathbf{A}}(\mathbf{r})$ is the vector potential of the electromagnetic field, $\hat{\mathbf{p}}$ is the canonical momentum of an electron, $\hat{\psi}^{\dagger}(\mathbf{r})$ ($\hat{\psi}(\mathbf{r})$) is electron creation (annihilation) operator.

Let $|\Phi_n\rangle$ be an eigenstate of $\hat{H}_{el}$ with eigenenergy E_n , $|N-\mu\rangle$ be a Fock state of the mode $\boldsymbol{\kappa}_0, s_0$ and $|\Psi_I\rangle$ be an eigenstate of $\hat{H}_{LD}$. $|\Psi_I\rangle$ can be represented as
$|\Psi_I\rangle$ can be represented as

$$|\Psi_I\rangle = \sum_{n,\mu} C^I_{n\mu} |\Phi_n\rangle |N-\mu\rangle. \tag{4}$$

Assuming that $\sqrt{N-\mu} \approx \sqrt{N}$, the Hamiltonian is

$$\begin{pmatrix}
\dots & \dots & \dots & \dots & \dots & \dots & \dots \\
\dots & \mathbf{E}+(N-2)\omega\mathbf{I} & \mathbf{T} & \mathbf{0} & \mathbf{0} & \mathbf{0} & \dots \\
\dots & \mathbf{T}^{\dagger} & \mathbf{E}+(N-1)\omega\mathbf{I} & \mathbf{T} & \mathbf{0} & \mathbf{0} & \dots \\
\dots & \mathbf{0} & \mathbf{T}^{\dagger} & \mathbf{E}+N\omega\mathbf{I} & \mathbf{T} & \mathbf{0} & \dots \\
\dots & \mathbf{0} & \mathbf{0} & \mathbf{T}^{\dagger} & \mathbf{E}+(N+1)\omega\mathbf{I} & \mathbf{T} & \dots \\
\dots & \mathbf{0} & \mathbf{0} & \mathbf{0} & \mathbf{T}^{\dagger} & \mathbf{E}+(N+2)\omega\mathbf{I} & \dots \\
\dots & \dots & \dots & \dots & \dots & \dots & \dots
\end{pmatrix},$$

where $\mathbf{E}$ is a diagonal matrix with the diagonal elements being the eigenenergies E_n of the $\hat{H}_{el}$, $\mathbf{I}$ and $\mathbf{0}$ are unit and zero matrices, correspondingly, $\mathbf{T}$ is a matrix with elements $T_{nn'}$, where

$$T_{nn'} = \sqrt{N\frac{2\pi}{V\omega}} \int d^3\mathbf{r} \langle \Phi_n | \hat{\psi}^{\dagger}(\mathbf{r}) e^{i\boldsymbol{\kappa}_0\mathbf{r}} \epsilon_{\kappa_0,s_0} \hat{\mathbf{p}} \hat{\psi}(\mathbf{r}) | \Phi_{n'} \rangle.$$

Further, we have to diagonalize this matrix. As it not possible to solve this problem for an infinite matrix, it's size has to be limited. Therefore, we introduce the notation μ_{max}, where $2\mu_{max}+1$ is the amount of blocks of the matrix.

Due to the periodicity property of the Hamiltonian the coefficients satisfy the following relation

$$C^{I_{\Delta\mu}}_{n,\mu} = C^{I_0}_{n,\mu+\Delta\mu}, \tag{5}$$

where I_0 is a reference state.

Thus, each Floquet eigenstate Ψ_{I_0} with an eigenvalue E_{I_0} has a "replica state" $\Psi_{I_{\Delta\mu}}$ with a corresponding eigenvalue $E_{I_{\Delta\mu}} = E_{I_0} + \Delta\mu\omega$. Therefore, physically different Floquet states can be characterized in the range $E \in [0, \omega]$.

2.2 Probe pulse

When the LD system is probed by means of high-energy nonresonant x-ray scattering the total Hamiltonian of the whole system is given by [3]

$$\hat{H} = \hat{H}_{LD} + \hat{H}_{\mathrm{x}} + \hat{H}_{\mathrm{x},int} \tag{6}$$

$$\hat{H}_{\mathrm{x}} = \sum_{\mathbf{k}_{\mathrm{x}},s_{\mathrm{x}}} \omega_{\mathbf{k}_{\mathrm{x}}} \hat{a}^{\dagger}_{\mathbf{k}_{\mathrm{x}},s_{\mathrm{x}}} \hat{a}_{\mathbf{k}_{\mathrm{x}},s_{\mathrm{x}}} \tag{7}$$

$$\hat{H}_{\mathrm{x},int} = \frac{1}{2c^2} \int d^3\mathbf{r} \hat{\psi}^{\dagger}(\mathbf{r}) \mathbf{A}^2_{\mathrm{x}}(\mathbf{r}) \hat{\psi}(\mathbf{r}) \tag{8}$$

where $\hat{H}_{\mathrm{x}}$ is the Hamiltonian of x-ray field, $\hat{H}_{\mathrm{x},int}$ is the interaction Hamiltonian between the electronic system and the x-ray field in a high-energy nonresonant regime, $\mathbf{A}_{\mathrm{x}}$ is the vector potential of the x-ray field. The probe x-ray pulse has a Gaussian shape

$$\mathcal{E}(t) = \sqrt{\frac{2\pi}{c} I_0} e^{-2ln2\frac{(t-t_0)^2}{\tau_p^2}}. \tag{9}$$

2.3 Basis

We diagonalize Hamiltonian $\hat{H}_{LD}$ of a laser-driven crystal using a basis

$$|\varphi_{m,\mathbf{k}}\rangle |N-\mu\rangle, \tag{10}$$

where $|\varphi_{m,\mathbf{k}}\rangle$ is an eigenstate of a one-body field-free Hamiltonian $\hat{H}_{el}$ of an electron in a crystal, $\mathbf{k}$ is a Bloch vector. According to the Bloch theorem, wave functions can be represented as

$$\varphi_{m,\mathbf{k}}(\mathbf{r}) = e^{i\mathbf{k}\mathbf{r}} u_{m,\mathbf{k}}(\mathbf{r}),$$
$$u_{m,\mathbf{k}}(\mathbf{r}) = u_{m,\mathbf{k}}(\mathbf{r}+\mathbf{R}).$$

One-body eigenstates of the Hamiltonian $\hat{H}$ are

$$|\phi_{i,\mathbf{k}}\rangle = \sum_{m,\mu} c^i_{m,\mathbf{k},\mu} |\varphi_{m,\mathbf{k}}\rangle |N-\mu\rangle \tag{11}$$

with energies $\varepsilon_{i,\mathbf{k}}$. The coefficients $c^i_{m,\mathbf{k},\mu}$ are the solutions of the equation

$$\sum_{m',\mu'} \langle\varphi_{m,\mathbf{k}}|\langle N-\mu|\hat{H}|N-\mu'\rangle|\varphi_{m',\mathbf{k}}\rangle c^i_{m',\mathbf{k},\mu'} = \varepsilon_{i,\mathbf{k}} c^i_{m,\mathbf{k},\mu}. \tag{12}$$

They also have a periodicity property

$$c^{i_0}_{m,\mathbf{k},\mu+\Delta\mu} = c^{i_{\Delta\mu}}_{m,\mathbf{k},\mu}. \tag{13}$$

2.4 Scattering probability

The probability of ultrafast x-ray scattering from a laser-driven crystal can be represented as the sum of two terms, namely, quasi-elastic and inelastic ones. Quasi-elastic means that an LD system in the Floquet state I_0 after interaction with light changes its state to a state $I_{\Delta\mu}$, in other words, the transitions only between physically equivalent replica states are taken into accoint. Wheareas, the inelastic term represents transitions between all non-replica states, namely from $I_{\Delta\mu}$ to $J_{\Delta\mu'}$, where $I_0 \neq J_0$.

$$P(\mathbf{G},\omega_{\kappa_s}) = P_{q.e.} + P_{ine.}, \tag{14}$$

$$P_{q.e.} = P_0 \Big| \sum_{i,\mathbf{k},m,m',\mu} c^{i*}_{m',\mathbf{k},\mu+\Delta\mu} c^{i}_{m,\mathbf{k},\mu} e^{i\Delta\mu\omega t_p} e^{-\frac{(\omega_{sh}+\Delta\mu\omega)^2\tau_p^2}{8ln2}} \mathcal{O}_{m'm}(\mathbf{k},\mathbf{G}) \Big|^2, \tag{15}$$

$$P_{ine.} = P_0 \sum_{i,j,\mathbf{k}} \Big| \sum_{\Delta\mu,m,m',\mu} c^{j*}_{m',\mathbf{k},\mu+\Delta\mu} c^{i}_{m,\mathbf{k},\mu} e^{i\Delta\mu\omega t_p} e^{-\frac{(\omega_{sh}+\varepsilon_{j,\mathbf{k}}-\varepsilon_{i,\mathbf{k}}+\Delta\mu\omega)^2\tau_p^2}{8ln2}} \mathcal{O}_{m'm}(\mathbf{k},\mathbf{G}) \Big|^2 \tag{16}$$

where i is an occupied one-body Floquet state, j in an unoccupied one,

$$\mathcal{O}_{m'm}(\mathbf{k},\mathbf{G}) = N_{cell} \int\limits_{u.c.} d^3\mathbf{r} u^{\dagger}_{m'\mathbf{k}}(\mathbf{r}) u_{m\mathbf{k}}(\mathbf{r}) e^{i\mathbf{G}\mathbf{r}},$$
$$P_0 = \frac{(8\pi)^2 I_0 \ln 2}{\tau_p^2 c} \frac{\sum\limits_{\mathbf{s}_s} |(\epsilon_{\kappa in}, \epsilon_{\kappa})|^2 \omega^2_{\kappa_s}}{(2\pi)^2 \omega^2_{in} c^3},$$
$$\omega_{sh} = \omega_{\kappa_s} - \omega_{in}.$$

$P_{q.e.}$ and $P_{ine.}$ represent quasi-elastic and inelastic scattering probability, correspondingly.

3 Analysis

We introduce the notations $\mathcal{G}(\omega) \equiv e^{-\frac{\omega^2\tau_p^2}{8\ln 2}}$ and $B_{\Delta\mu} \equiv \sum\limits_{i,\mathbf{k},m,m',\mu} c^{i*}_{m',\mathbf{k},\mu+\Delta\mu} c^{i}_{m,\mathbf{k},\mu} \mathcal{O}_{m'm}(\mathbf{k},\mathbf{G})$.

3.1 Time-unresolved signal

In this work, we study how the expression for the scattering probability in Eq. (15) changes for long probe pulses. The time-independent part of the quasi-elastic term can be represented as

$$P^{indep}_{q.e.} = P_0 \sum_{\Delta\mu} \Big| B_{\Delta\mu} \Big|^2 \mathcal{G}(2(\omega_{sh} + \Delta\mu\omega)). \tag{17}$$

The time-dependent part of the quasi-elastic term can be represented as

$$P_{q.e.} = P_0 \sum_{\Delta\mu} \sum_{\delta\neq 0} B_{\Delta\mu} B^*_{\Delta\mu+\delta} e^{-i\delta\omega t} \mathcal{G}(\omega_{sh} + \Delta\mu\omega) \mathcal{G}(\omega_{sh} + \Delta\mu\omega + \delta\omega). \tag{18}$$

Let us consider a probe pulse with duration τ_p such that Gaussian functions $\mathcal{G}(\omega_{sh})$ and $\mathcal{G}(\omega_{sh} + \delta\omega)$ do not overlap with each other for every $\delta \neq 0$, so that their product is zero. This leads to

$$P^{dep}_{q.e.} = 0. \tag{19}$$

Finally,

$$\boxed{P_{q.e.} = P_0 \sum_{\Delta\mu} \Big| N_{cell} \int\limits_{u.c.} d^3\mathbf{r} \tilde{\rho}(\mathbf{r}, \Delta\mu) e^{i\mathbf{G}\mathbf{r}} \Big|^2 e^{-\frac{(\omega_{sh}+\Delta\mu\omega)^2\tau_p^2}{4ln2}}}, \tag{20}$$

where

$$\begin{aligned} \tilde{\rho}(\mathbf{r}, \Delta\mu) &= \langle \Psi_{I_{\Delta\mu}} | \hat{\psi}^{\dagger}(\mathbf{r}) \hat{\psi}(\mathbf{r}) | \Psi_{I_0} \rangle \\ &= \sum_{i,\mathbf{k}} \sum_{m,m',\mu} c^{i*}_{m'.\mathbf{k},\mu+\Delta\mu} c^{i}_{m.\mathbf{k},\mu} u^{\dagger}_{m',\mathbf{k}}(\mathbf{r}) u_{m,\mathbf{k}}(\mathbf{r}). \end{aligned} \tag{21}$$

3.1.1 Electron density

Electron density of the LD system can be represented as

$$\rho(\mathbf{r},t)=\sum_{\Delta\mu}e^{i\Delta\mu\omega t}\tilde{\rho}(\mathbf{r},\Delta\mu). \tag{22}$$

Let us show that $\rho(\mathbf{r},t)$ is real. In expression for $\tilde{\rho}(\mathbf{r},-\Delta\mu)$ we substitute $\mu\to\mu+\Delta\mu$.

$$\begin{aligned}\tilde{\rho}(\mathbf{r},-\Delta\mu)&=\sum_{i,\mathbf{k},m,m',\mu}c^{i*}_{m'\mathbf{k}\mu-\Delta\mu}c^{i}_{m\mathbf{k}\mu}u^{\dagger}_{m'\mathbf{k}}(\mathbf{r})u_{m\mathbf{k}}(\mathbf{r})\\&=\sum_{i,\mathbf{k},m,m',(\mu+\Delta\mu)}c^{i*}_{m'\mathbf{k}\mu}c^{i}_{m\mathbf{k}\mu+\Delta\mu}u^{\dagger}_{m'\mathbf{k}}(\mathbf{r})u_{m\mathbf{k}}(\mathbf{r}).\end{aligned} \tag{23}$$

Since μ changes from $-\infty$ to $+\infty$, and substituting $m\to m', m'\to m$, we obtain

$$\tilde{\rho}(\mathbf{r},-\Delta\mu)=\sum_{i,\mathbf{k},m,m',\mu}c^{i*}_{m'\mathbf{k}\mu}c^{i}_{m\mathbf{k}\mu+\Delta\mu}u^{\dagger}_{m'\mathbf{k}}(\mathbf{r})u_{m\mathbf{k}}(\mathbf{r}) \tag{24}$$

$$=\sum_{i,\mathbf{k},m,m',\mu}c^{i*}_{m\mathbf{k}\mu}c^{i}_{m'\mathbf{k}\mu+\Delta\mu}u^{\dagger}_{m\mathbf{k}}(\mathbf{r})u_{m'\mathbf{k}}(\mathbf{r}) \tag{25}$$

$$=\Big(\sum_{i,\mathbf{k},m,m',\mu}c^{i}_{m\mathbf{k}\mu}c^{i*}_{m'\mathbf{k}\mu+\Delta\mu}u_{m\mathbf{k}}(\mathbf{r})u^{\dagger}_{m'\mathbf{k}}(\mathbf{r})\Big)^{\dagger} \tag{26}$$

$$=\tilde{\rho}(\mathbf{r},\Delta\mu)^{\dagger}. \tag{27}$$

Thus,

$$\boxed{\tilde{\rho}(\mathbf{r},-\Delta\mu)=\tilde{\rho}(\mathbf{r},\Delta\mu)^{\dagger}}. \tag{28}$$

Thus, we conclude that the electron density $\rho(\mathbf{r},t)=\sum\limits_{\Delta\mu}e^{i\Delta\mu\omega t}\tilde{\rho}(\mathbf{r},\Delta\mu)$ is real as it should be.

3.1.2 Calculation parameters

If not stated differently, all the below is studied for the Bragg peak $\mathbf{G}=(0,0,2)$, probe-pulse duration $\tau_p=6$ fs, pump-pulse frequency $\omega=1.55$ eV, pump-pulse polarization $\mathbf{e}=(0,0,1)$ and pump-pulse intensity $I_0=2\cdot10^{12}\frac{W}{cm^2}$.

3.1.3 Convergence study

In order to obtain the wave functions in Eq. (4), we need to diagonalize the Hamiltonian in the Floquet-Bloch representation, which is an infinite matrix. To solve this problem by numerical calculations, we need to limit the size of the matrix by some finite integer. The question is how big the matrix should be to represent the true physical behavior of the system. For this reason we make a convergence study with respect to $\mu_{\max}$, which determines the amount of blocks of the Hamiltonian matrix. We also investigate, how many conduction bands of the crystal, we should take into account.

First, we study the minimum required number of conduction bands. Figure 1 shows the plot of the scattering signal from electrons in the MgO crystal taking into account 10, 15 and 20 conduction bands.

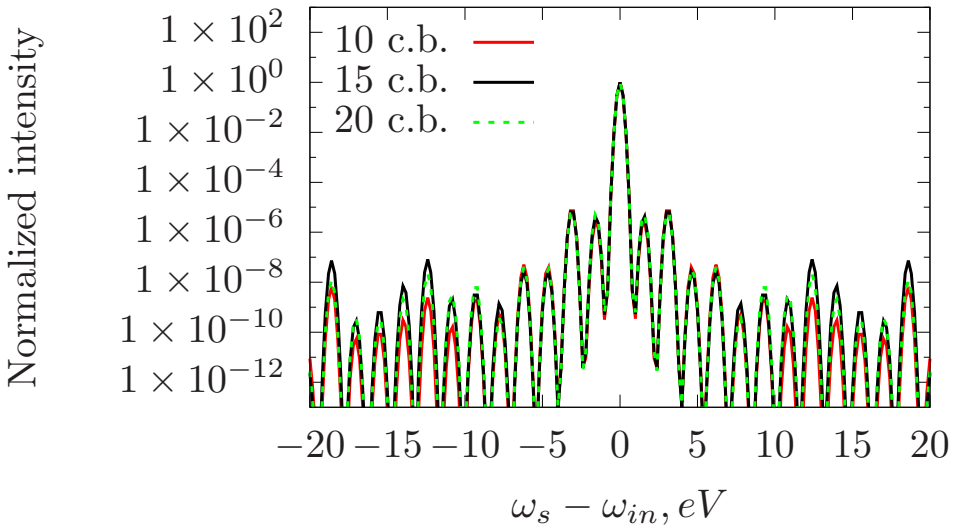

Figure 1: Convergence study with respect to the number of conduction bands (c.b.)

It follows from Figure 1 that signals calculated with 15 and 20 conduction bands almost coincide. Thus, we will use 15 conduction band for further calculations.

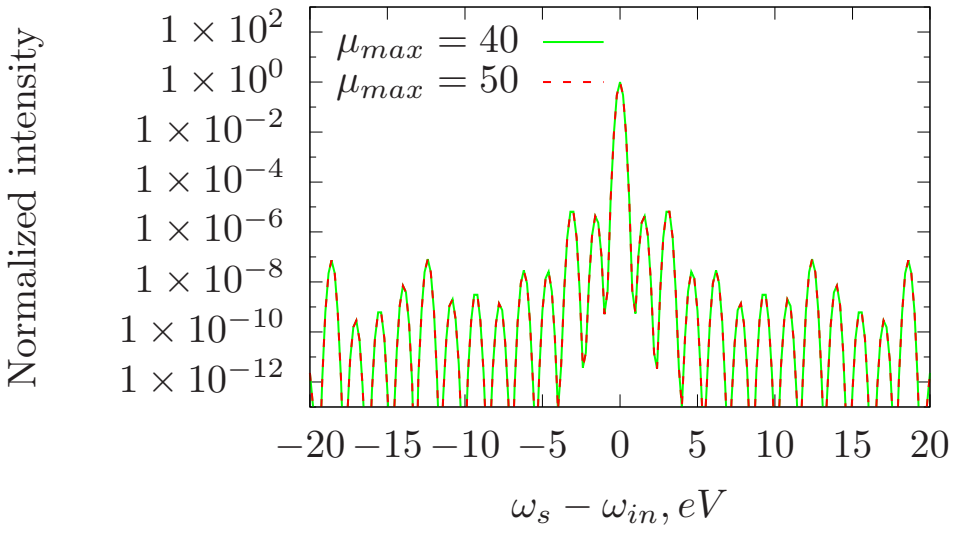

Figure 2: Convergence study with respect to μ_{max}

For 15 conduction bands, we make a convergence study with respect to $\mu_{\max}$. From Figure 2, we conclude that the calculation is converged for $\mu_{max} = 40$. Thus, we will use this value for further calculations.

Now we study the inelastic scattering case. Figure 3 shows the plots of the inelastic signals for different number of conduction bands.

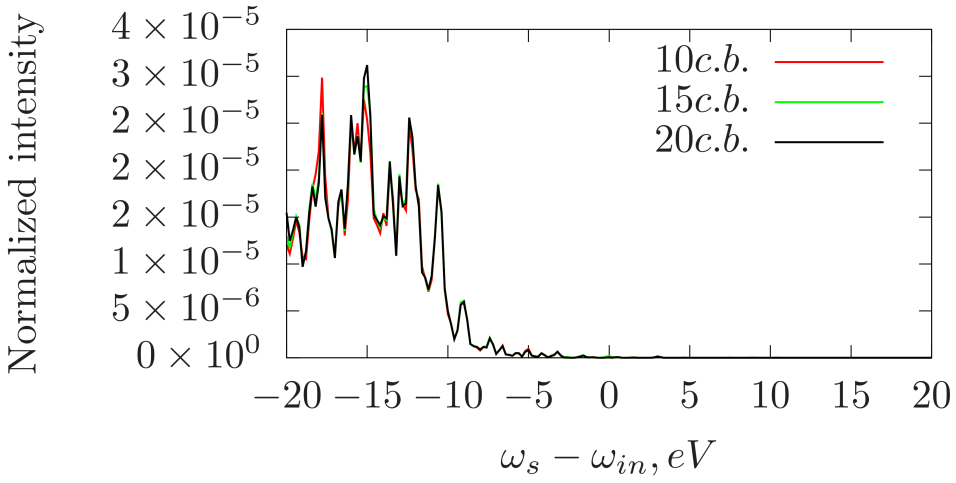

Figure 3: Convergence study with respect to the number of conduction bands (c.b.)

We see from Figure 3 that the inelastic signal converges faster for lower energies. The inelastic signal induced by the transitions from valence bands to conduction bands. The signal for higher energies comparing to the signal for smaller energies is much more sensitive to the number of the conduction bands we take into account.

3.1.4 Time evolution

$T = \frac{2\pi}{\omega}$ is the time period of the optical field oscillation. As you one can see from Eq. (22), ω is also a period of the electron density oscillation. Evolution in time for the quasi-elastic and the inelastic signals are represented in Figure 4.

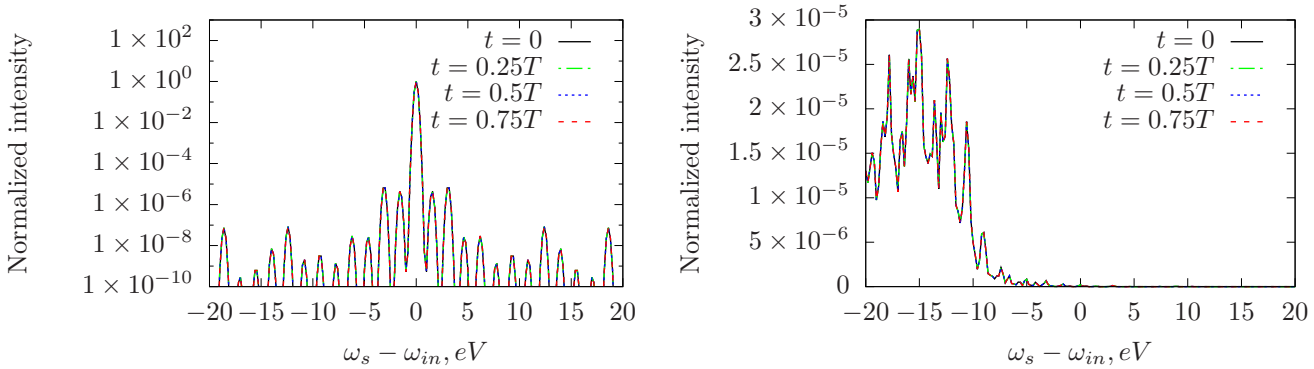

Figure 4: (a) Time evolution of the quasi-elastic signal. (b) Time evolution of the inelastic signal.

As we can see from Figure 4, there is no time dependence for the quasi-elastic scattering term as well as for the inelastic one. Thus, the total probability (intensity) do not evolve in time for the probe-pulse duration of 6 fs.

3.1.5 Dependence on the pump-pulse intensity

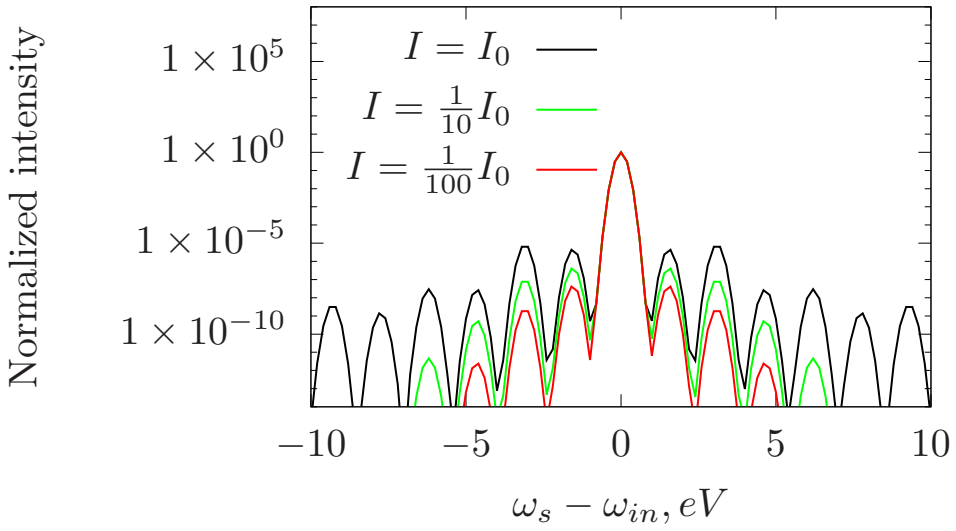

Figure 5: Dependence of the quasi-elastic signal on the pump-pulse intensity. $I_0 = 2 \cdot 10^{12} \frac{W}{cm^2}$.

We study how the signal changes for different intensities of the pump pulse. As we can see from Figure 5, the intensities of the peaks monotonically decrease with the order of the peaks at low intensities of the pump pulse. Thus, the interaction between the pump pulse and the electronic structure of the crystal can be described within the perturbation theory. Whereas, at higher intensities the Floquet's theory is necessary.

3.1.6 Symmetry

Let us study the symmetry property of the signals. One can see from Figures 1, 2 and 4a that the quasi-elastic signal is symmetric with respect to $\omega_s - \omega_{in}$. However, the inelastic signal is not symmetric as follows from Figures 3 and 4b. In an inelastic scattering process, the energy of the electronic system is increased and the signal is located in $\omega_s - \omega_{in} < 0$ area. We compare the quasi-elastic and inelastic signals for $\mathbf{G}$ and $-\mathbf{G}$ on Figure 6. As we can see, signals on Figure 6 are absolutely equal for both $\mathbf{G}$ and $-\mathbf{G}$.

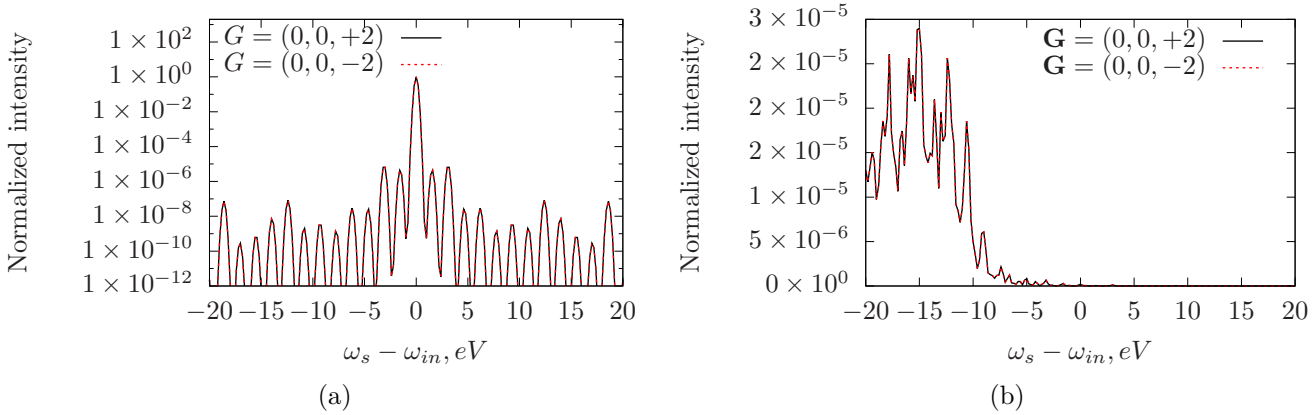

Figure 6: Signals corresponding $\mathbf{G} = (0, 0, 2)$ and $\mathbf{G} = (0, 0, -2)$ Bragg vectors. (a) The quasi-elastic signal. (b) The inelastic signal.

3.1.7 Pulse duration

Let us study how the signal changes with respect to the probe pulse duration. We consider three different values of the pulse duration $\tau_p = 6$ fs,$\tau_p = 9$ fs,$\tau_p = 12$ fs and draw the plots for the quasi-elastic, inelastic and total signals.

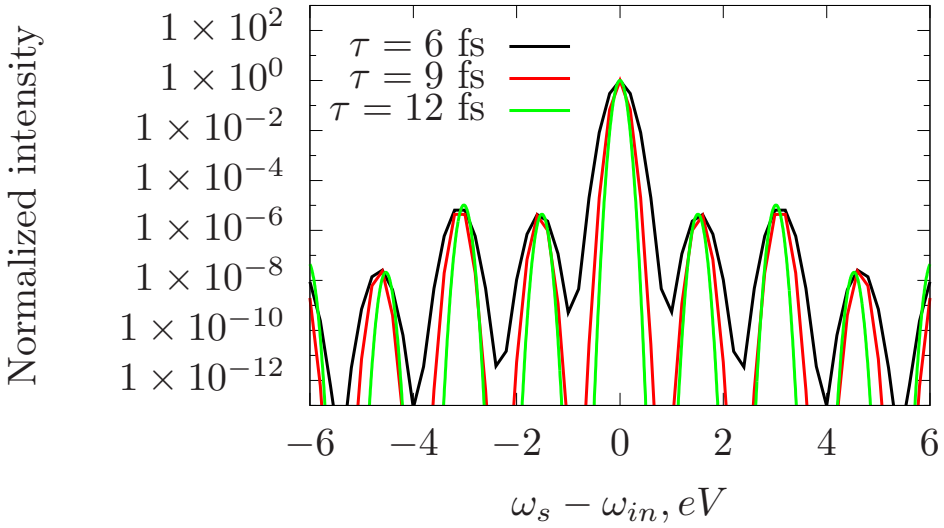

Figure 7: The quasi-elastic signals for different probe pulse durations.

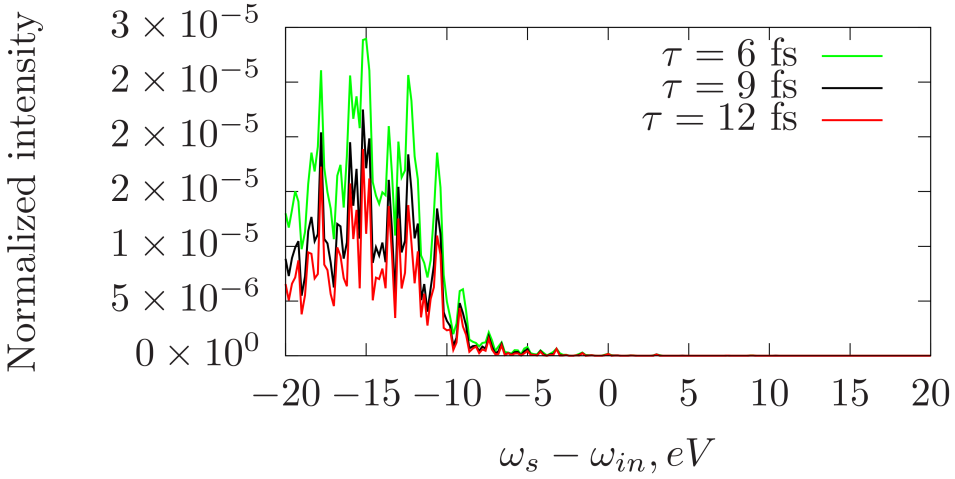

Figure 8: The inelastic signals for different probe pulse durations.

From plots in Figure 7, we see that on the peaks in the quasi-elastic signal become more narrow and distinguishable. It follows from Figure 8 that the inelastic part of the signal decreases while the pulse duration increases.

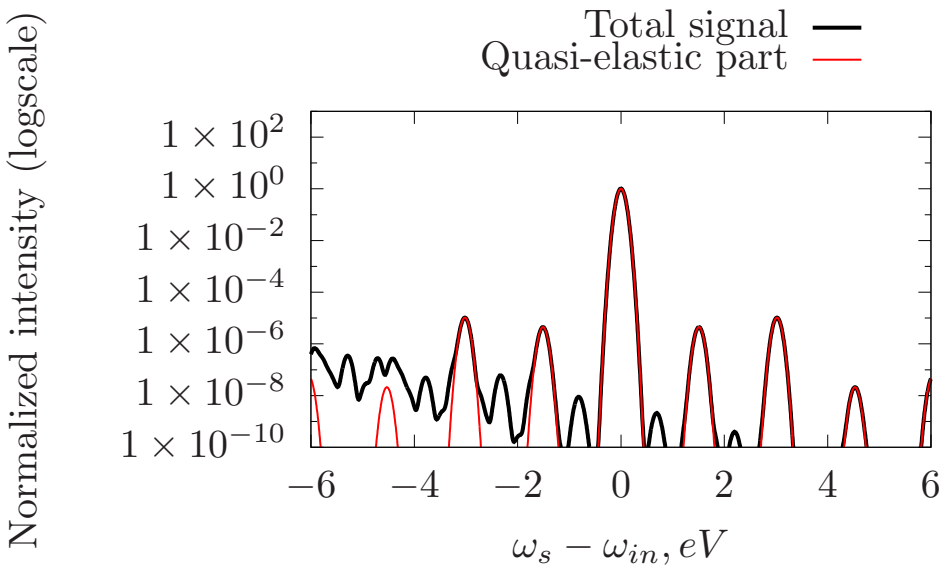

Figure 9: The total signal and quasi-elastic part of it at pulse duration $\tau_p = 12$ fs

Let us compare the total signal and quasi-elastic part of the signal on Figure 9. We study how the difference between the total signal and the quasi-elastic part will change in respect to probe pulse duration. We compare the intensities of the first, second and third peaks corresponding to $\omega_{\text{in}} - 1.55$ eV, $\omega_{\text{in}} - 3.1$ eV and $\omega_{\text{in}} - 4.65$ eV scattering energies. Figures 10, 11 and 12 show the ratios between the total signal and the quasi-elastic part of the signal for the first, second and third peaks. From Figures 10 and 11 we conclude that the total signal and the quasi-elastic signal at $\omega\text{in} - \omega$ and $\omega\text{in} - 2\omega$ almost coincide for probe-pulse durations $\tau > 24$ fs. This means that the inelastic signal can be spectroscopically separated from the quasi-elastic signal at these probe-pulse durations. We can not make such a conclusion from Figure 12 because the intensity of the peak is too small.

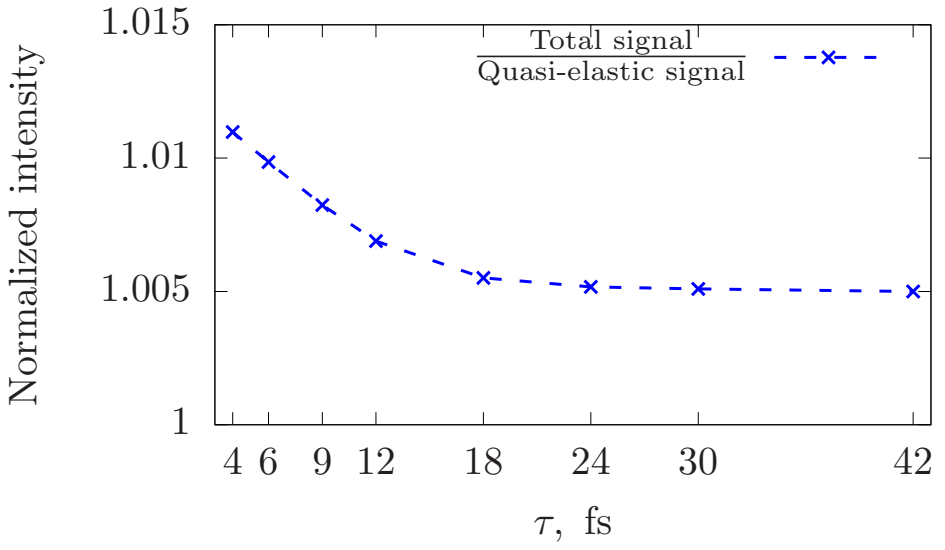

Figure 10: The ratio of the total signal to the quasi-elastic one for the first peak ($\omega = 1.55$) depending on the probe-pulse duration.

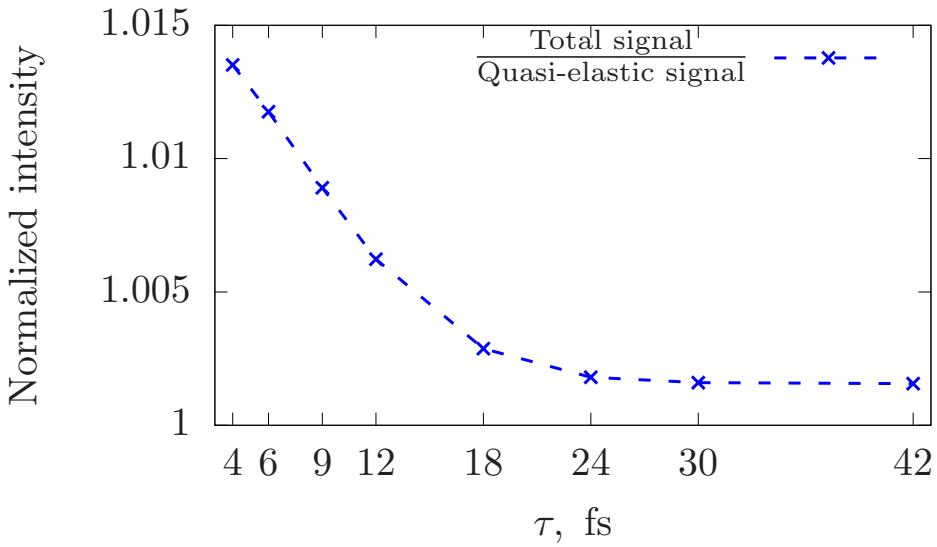

Figure 11: The ratio of the total signal to the quasi-elastic one for the second peak ($\omega = 3.1$) depending on the probe-pulse duration.

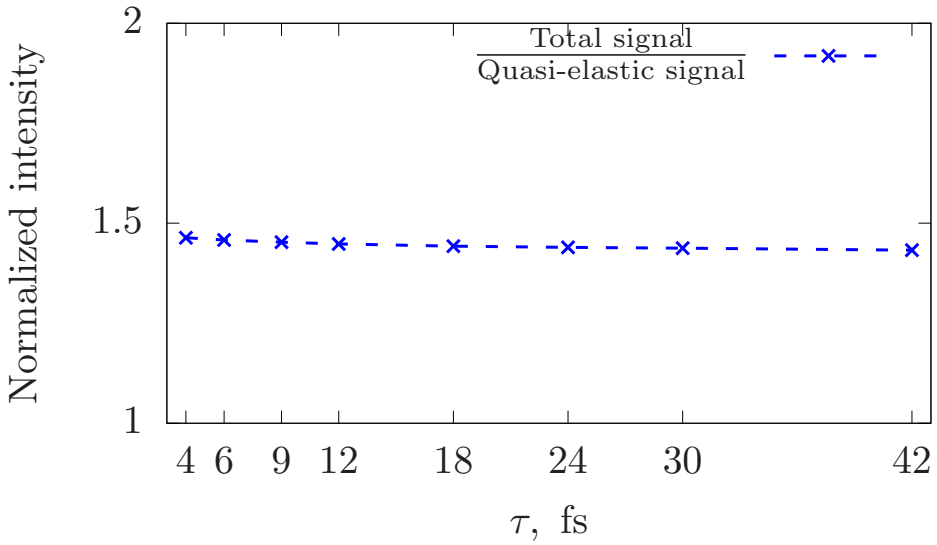

Figure 12: The ratio of the total signal to the quasi-elastic one for the third peak ($\omega = 4.65$) depending on the probe-pulse duration.

3.1.8 Polarization

Let us now consider how the signal depends on the pump pulse polarization. The vector $\mathbf{e}$ represents the pump pulse polarization. We study how the quasi-elastic part of the signal changes with respect to the polarization vector $\mathbf{e} = (\cos\varphi, 0, \sin\varphi)$ where $\varphi \in [0, 90]$. Figure 13 shows the dependence of the intensity of the first-order quasielastic Bragg peak on the angle φ.

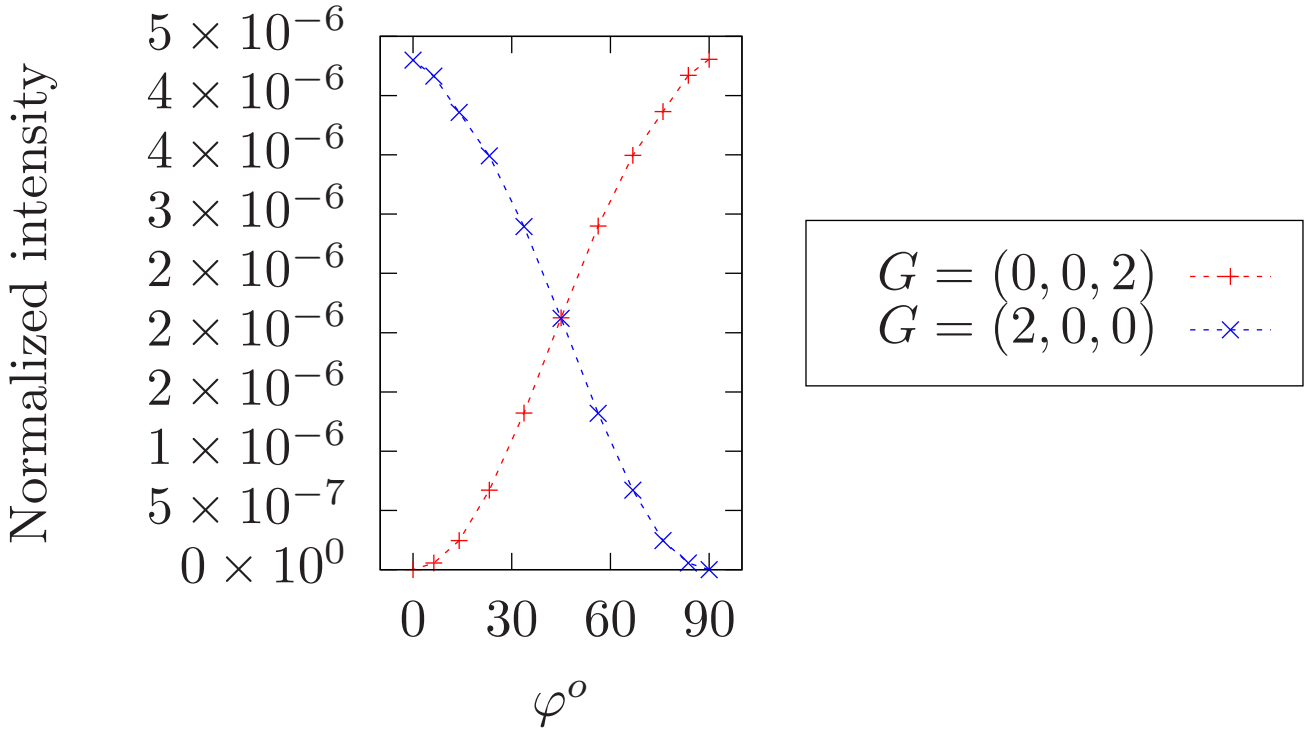

Figure 13: The dependence of the first-peak intensity of the quasi-elastic part of the signal on the polarization of the pump pulse $\mathbf{e} = (\cos\varphi, 0, \sin\varphi)$

The behavior can be described by an analytical function. For instance, the dependence for $\mathbf{G} = (2, 0, 0)$ first peak can be represented as $I(\varphi) = 4.3{\cdot}10^{-6}\cos^2\varphi$. Figure 14 and 15 show the dependence of the intensity of the second-order and the third-order quasi-elastic Bragg peak on the angle φ.

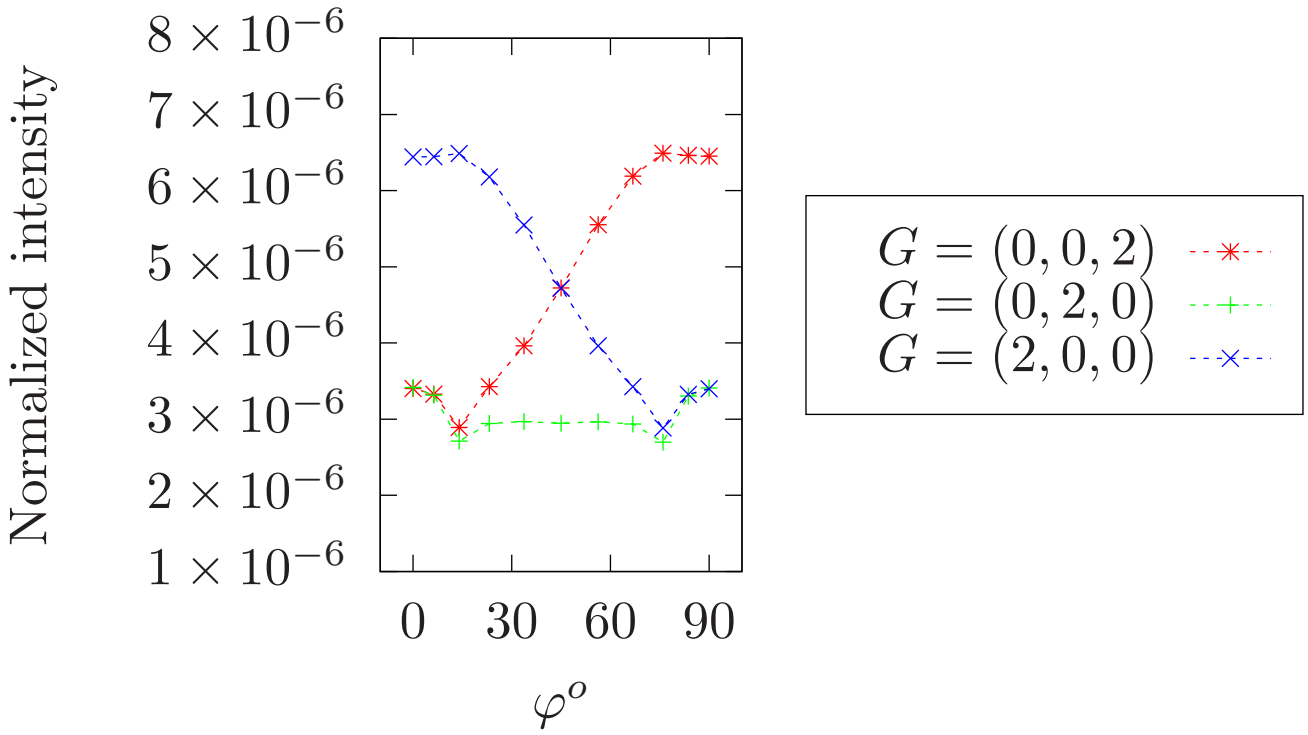

Figure 14: The dependence of the second-peak intensity of the quasi-elastic part of the signal on the polarization of pump pulse $\mathbf{e} = (\cos\varphi, 0, \sin\varphi)$.

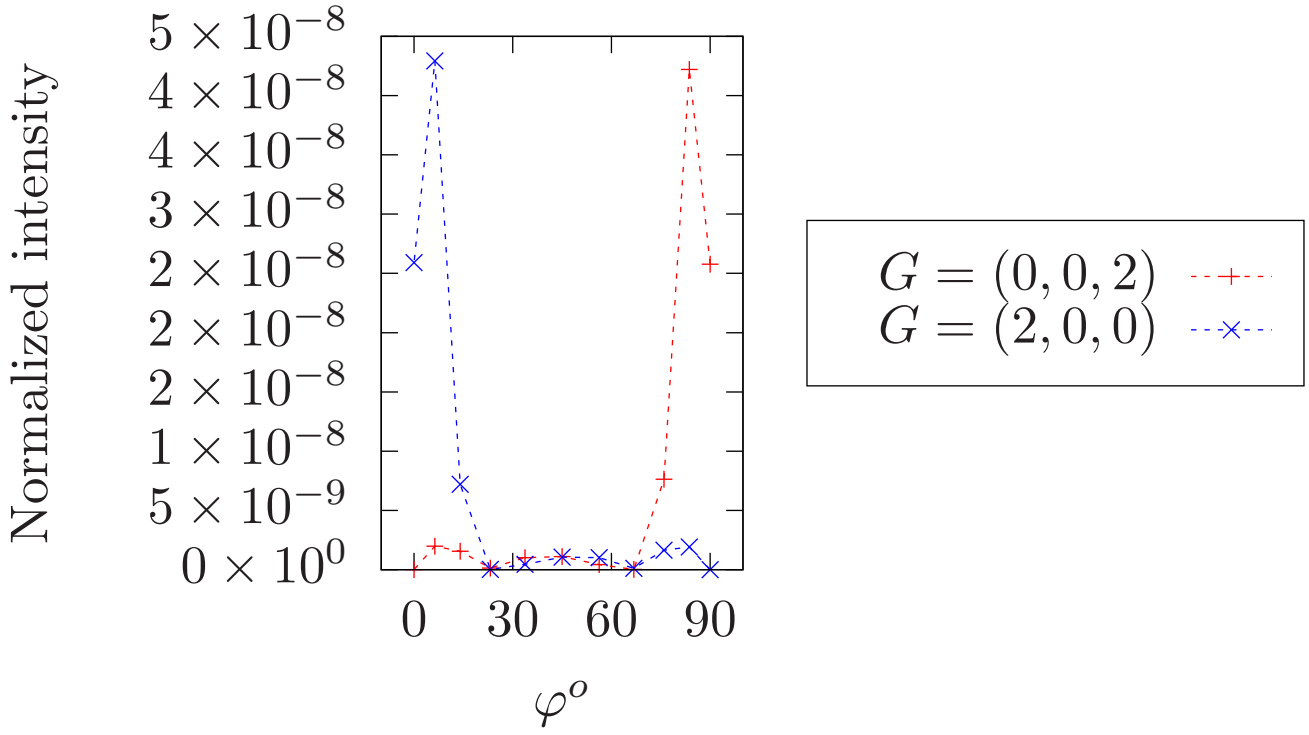

Figure 15: The dependence of the third-peak intensity of the quasi-elastic part of the signal on the polarization of pump pulse $\mathbf{e} = (\cos\varphi, 0, \sin\varphi)$.

3.1.9 Pump pulse frequency

We study how the signal depends on the pump-pulse frequency. Figures 16 and 17 show the quasi-elastic and the inelastic signals at two pump-pulse frequencies: $\omega = 1.55$ eV and $\omega = 3.1$ eV.

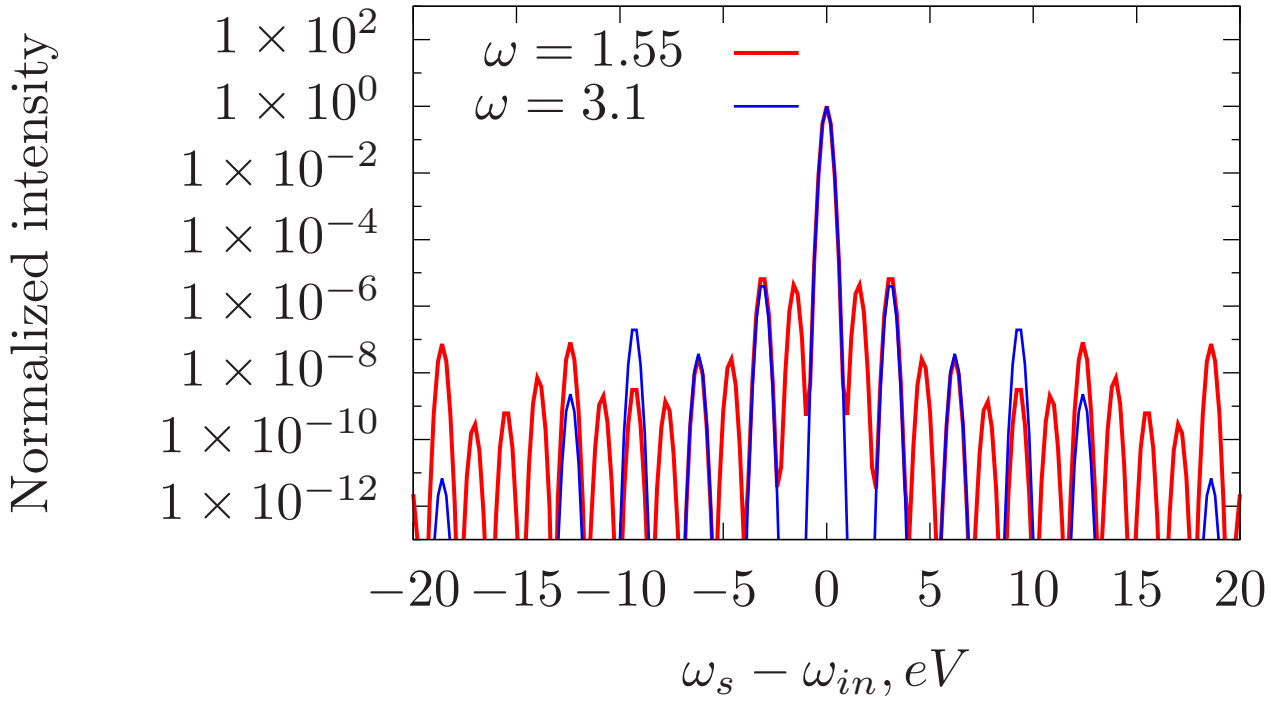

Figure 16: The quasi-elastic part of the signal at two pump-pulse frequencies of 1.55 eV and 3.1 eV.

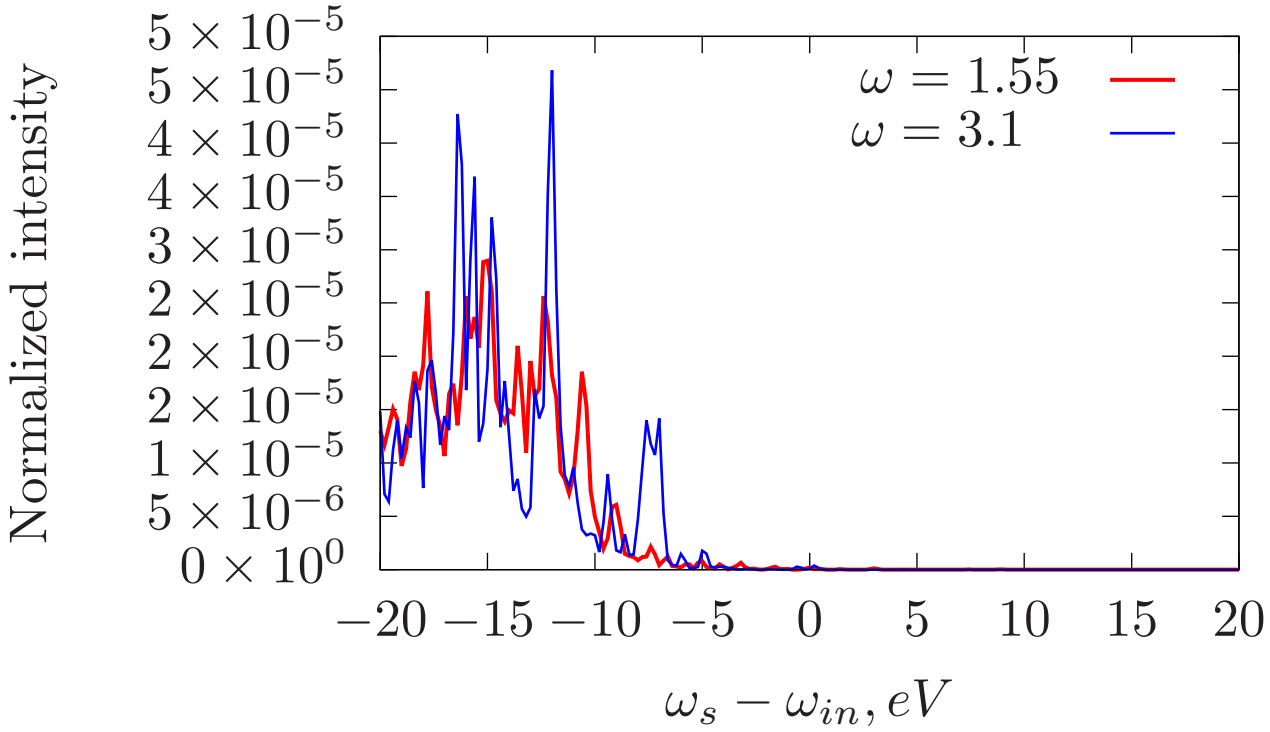

Figure 17: The inelastic part of the signal at two pump-pulse frequencies of 1.55 eV and 3.1 eV.

3.2 Time-resolved signal

The quasi-elastic part of the scattering probability can be represented as

$$P_{q.e.} = P_0 \sum_{\Delta\mu} \sum_{\delta} B_{\Delta\mu} B^*_{\Delta\mu+\delta} e^{-i\delta\omega} \mathcal{G}(\omega_{sh} + \Delta\mu\omega) \mathcal{G}(\omega_{sh} + \Delta\mu\omega + \delta\omega). \tag{29}$$

As one can see, the time-dependent part is determined by the product of two Gaussian functions. Depending on the pulse duration τ_p, the product of two Gaussian functions could be zero or not zero. There are two limit cases. The first one is defined by

$$\mathcal{G}(\omega_{sh}) \mathcal{G}(\omega_{sh} + \delta\omega) \approx \mathcal{G}^2(\omega_{sh}) = \mathcal{G}(2\omega_{sh}) \tag{30}$$

for $\delta \leq \delta_1$.
It means that we can not distinguish the positions of two Gaussians. The second one is defined by

$$\mathcal{G}(\omega_{sh}) \mathcal{G}(\omega_{sh} + \delta\omega) \approx 0 \tag{31}$$

for $\delta > \delta_2$. With these limits, the quasi-elastic probability can be represented as

$$\begin{aligned} P_{q.e.} = P_0 \mathcal{G}(2\omega_{sh}) \sum_{|\delta|=0}^{\delta_1} \Big(\sum_{\Delta\mu} B_{\Delta\mu} B^*_{\Delta\mu+\delta} e^{-i\delta\omega t} \Big) + \\ + P_0 \sum_{|\delta|=\delta_1+1}^{\delta_2} \Big(\sum_{\Delta\mu} B_{\Delta\mu} B^*_{\Delta\mu+\delta} e^{-i\delta\omega t} \mathcal{G}(\omega_{sh} + \Delta\mu\omega) \mathcal{G}(\omega_{sh} + \Delta\mu\omega + \delta\omega) \Big) \end{aligned} \tag{32}$$

The dependence of limits δ_1 and δ_2 on τ_p and ω is the following:

$$\delta_1 = mod\Big(\frac{4.3}{\omega\tau_p}\Big) \quad \delta_2 = mod\Big(\frac{5.1}{\omega\tau_p}\Big) \tag{33}$$

Examples for $\omega = 1.55$ eV are:

$$\begin{aligned} &\text{for } \tau_p = 1 \text{ fs}, \ \delta_1 = 2 \quad \delta_2 = 4, \\ &\text{for } \tau_p = 0.4 \text{ fs}, \ \delta_1 = 6 \quad \delta_2 = 9, \\ &\text{for } \tau_p = 0.1 \text{ fs}, \ \delta_1 = 27 \quad \delta_2 = 33. \end{aligned}$$

For $\tau_p > 3.3$ fs $\rightarrow \delta_2 = 1$ and the probability $P_{q.e.}$ becomes time-independent. This case was studied in Section "time-unresolved signal".

The time evolution of the signal from $\frac{1}{2}T$ to T repeats the evolution from 0 to $\frac{1}{2}T$ in the opposite direction as demonstrated on Figure 18. Thus, we observe the time evolution of the system within the interval $[0, \frac{1}{2}T]$. Assuming the probe-pulse duration $\tau_p = 1$ fs , we calculate the time evolution of the scattering signals at different $\mathbf{G}$ vectors. Figure 19 shows how the quasi-elastic signal evolves in time for both $\mathbf{G} = (0, 0, 2)$ and $\mathbf{G} = (0, 0, -2)$ Bragg peaks.

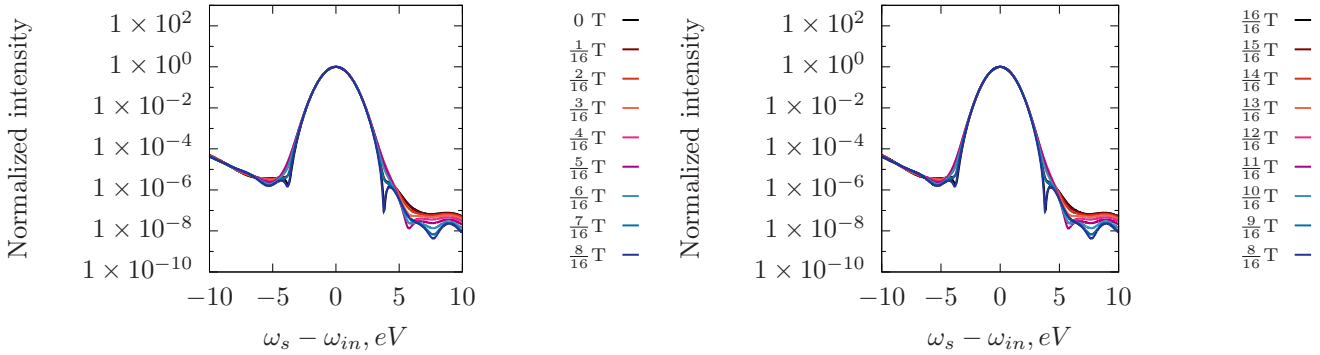

(a) (b)

Figure 18: The time evolution of the total signal (a) from 0 to $\frac{1}{2}T$ and (b) from $\frac{1}{2}T$ to T.

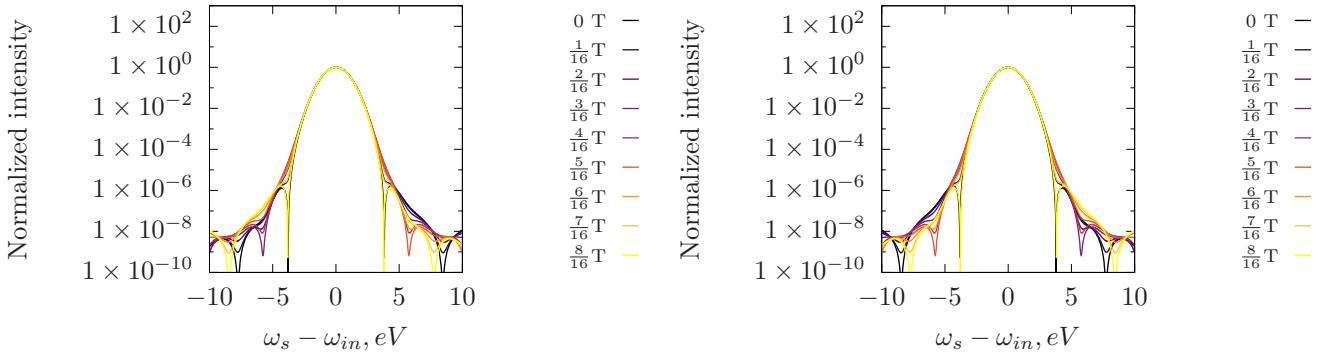

(a) (b)

Figure 19: The time evolution of the quasi-elastic signal from from 0 to $\frac{1}{2}$T for (a) $\mathbf{G} = (0, 0, 2)$ and (b) $\mathbf{G} = (0, 0, -2)$.

In order to take a closer look on the time evolution of the scattering signal, let us study on Figure 20 the difference between the two quasi-elastic signals shown on Figure 19.

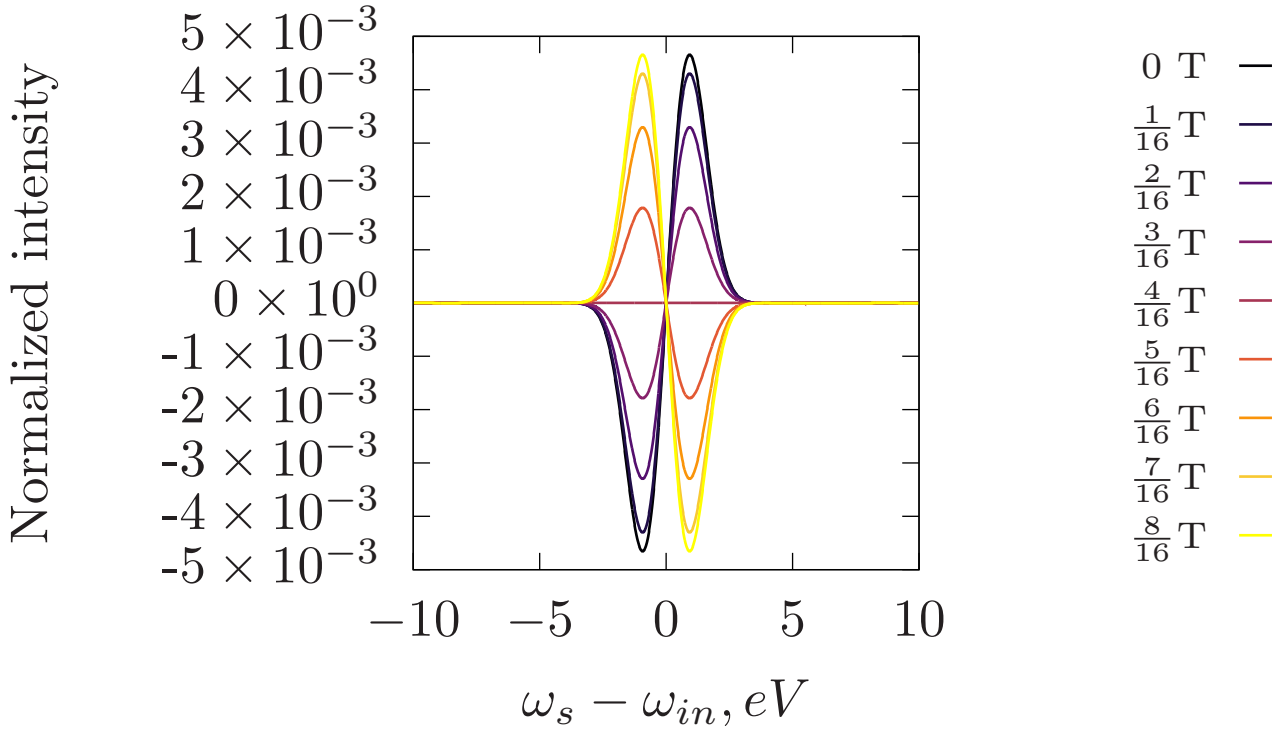

Figure 20: The difference between the quasi-elastic part of the signals with $\mathbf{G} = (0, 0, 2)$ and $\mathbf{G} = (0, 0, -2)$.

As one can see, the quasi-elastic signal for Bragg peak $\mathbf{G} = (0, 0, -2)$ in the time moment t_p is equal to the quasi-elastic signal for Bragg peak $\mathbf{G} = (0, 0, 2)$ in the time moment $t_p + \frac{1}{2}T$. The same conclusion can be made for the inelastic signal as can be seen from Figures 21 and 22. Figure 23 shows how the total signal evolves in time for both $\mathbf{G} = (0, 0, 2)$ and $\mathbf{G} = (0, 0, -2)$ Bragg peaks.

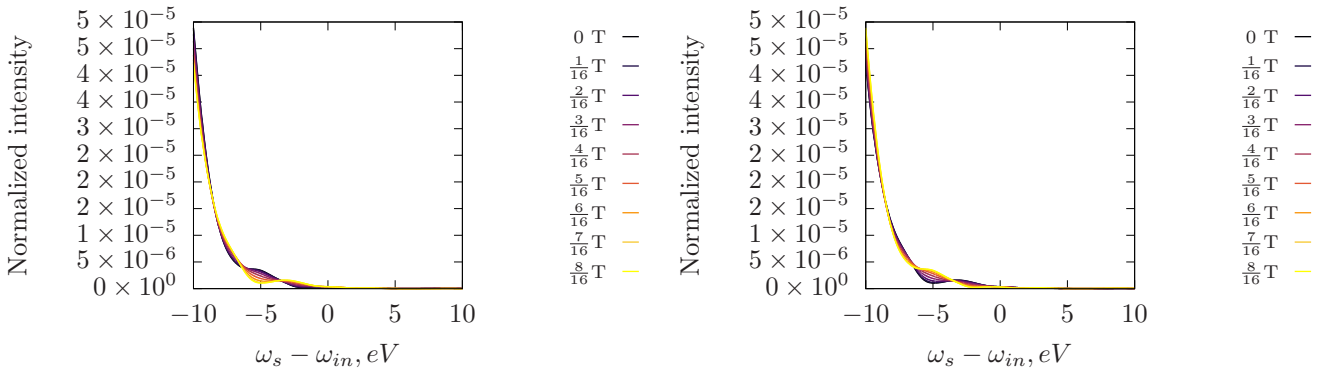

Figure 21: The inelastic signals at different time points. (a) Signal corresponding to $\mathbf{G} = (0, 0, 2)$. (b) Signal corresponding to $\mathbf{G} = (0, 0, -2)$.

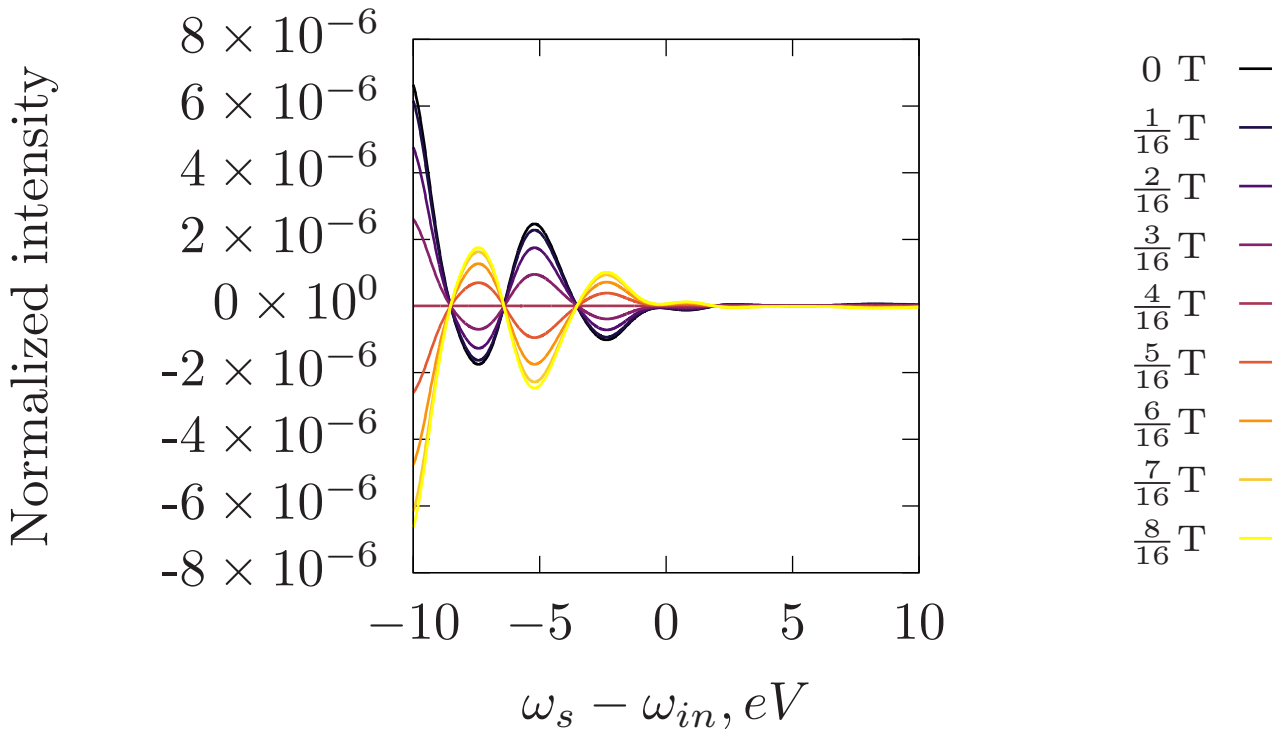

Figure 22: The difference between the inelastic part of the signals with $\mathbf{G} = (0, 0, 2)$ and $\mathbf{G} = (0, 0, -2)$.

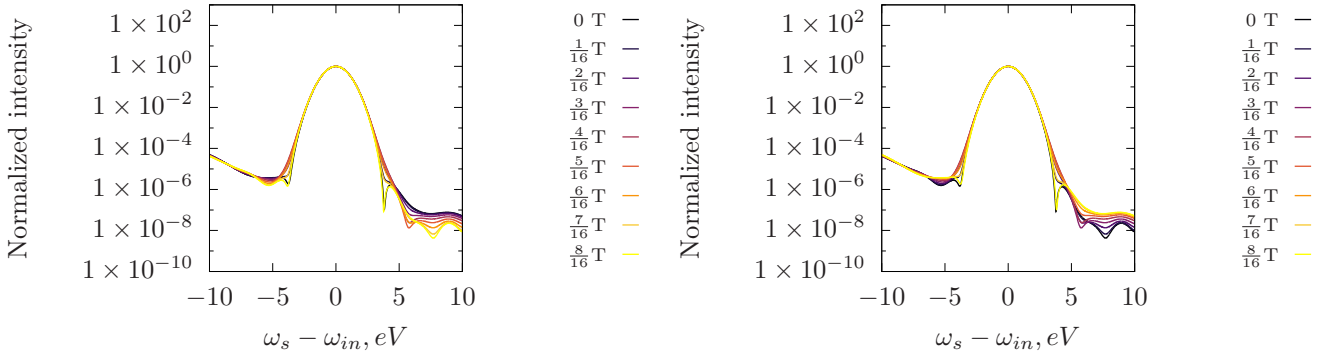

(a) (b)

Figure 23: The time evolution of the total signal from from 0 to $\frac{1}{2}$T for (a) $\mathbf{G} = (0, 0, 2)$ and (b) $\mathbf{G} = (0, 0, -2)$.

4 Conclusion

We studied ultrafast x-ray scattering from a laser-drivel MgO crystal. The signal dependence on significant parameters of the laser-driven system and probe pulse was shown. The dependence on pump pulse polarization, frequency and intensity were shown. In particular, we demonstrated that the probe-pulse duration determine the time-resolution of the signal.

Acknowledgment

Author is deeply grateful to his supervisor Daria Gorelova who has been the significant support throughout the entire project. I express special gratitude to Robin Santra for useful discussions and for the opportunity to develop this project at the CFEL-DESY Theory Division. Also, I thank the whole DESY summer school organization team.

References

[1] H. Hsu, L.E. Reichl, Phys. Rev. B **74**, 115406 (2006)

[2] J.H.Shirley, Phys. Rev. **138**, B979 (1965)

[3] D. Popova-Gorelova, D.A. Reis, R. Santra, Submitted, (2018)